IN-SITU ULTRASONIC IMAGING OF PRINTED ELECTRONICS INK DEPOSITION AND CURING

Anuj Baskota[1], Landon Ivy[2], Carlos Ospina[3], Justin Kuo[1], Juneho Hwang[2], Ved Gund[2], Benyamin Davaji[2,4], Peter Doerschuk[2,5], and Amit Lal[1,2]

[1]Geegah Inc., Ithaca, USA. [2]School of Electrical and Computer Engineering, Cornell University, Ithaca, USA. [3]BotFactory Inc, USA. [4]Department of Electrical and Computer Engineering, Northeastern University, Boston, USA. and [5]Meinig School of Biomedical Engineering, Cornell University, Ithaca, USA.

ABSTRACT

We report the first-ever in-situ imaging of 3D-Printed Electronics (PE) ink delivery and drying during the printing using GHz ultrasonic imager. The CMOS integrated GHz ultrasonic technology consists of a 128 x 128-pixel array of Aluminum Nitride transducers that image the surface of the silicon chip with transmit/receive of short ultrasonic pulses. The reflected US pulses measure crucial ink parameters such as ink's acoustic impedance and temperature at a sampling rate of up to 30 frames per second. We demonstrate the observation of ink droplets delivered to a surface, the creation of secondary droplets on the surface, and the time history of the ink curing process. The data at single pixel and images over a collection of images indicates that the GHz imager can be used to provide real-time quantitative feedback on the printing process, thus providing uniform and higher yield PE devices.

KEYWORDS

GHz, ultrasonic imaging, quality control, printed electronics, 3D printing, conductive ink, insulating ink

INTRODUCTION

Printed Electronics (PE) hardware has enabled the rapid development of passive/active circuit components, flexible wearables, diodes, and smart systems with a variety of sensing applications [1]. Over the traditional photolithography fabrication process, PE holds significant advantages in production speed, cost, material usage, flexibility in the substrate choice, and carbon footprint [2]. Although there is a remarkable research and development progress of PE devices, there are still several challenges that have limited its mass manufacturing potential. While printing resolution, uniformity of printed layers, and process stability are a few limitations for PE, one of the major drawbacks is the lack of optimum quality control during the printing process [3].

There are several factors such as ink quality (density, viscosity) and temperature (ink, substrate, and surrounding air) that must be appropriately decided to achieve proper ink adhesion, spread, and drying on the substrate surface [4]. Optical imaging using microscopes has been used for determining film delivery accuracy. Optical imaging generally requires a larger footprint requiring a light source and lensing. Further, optical imaging is only applicable to reflective surfaces, which is difficult for transparent inks. Furthermore, optical imaging also does not allow the imaging of mechanical and thermal properties of the ink. Monitoring the morphology as well as several material properties of ink film deposited on the substrate is necessary to understand the quality of the print. Some imaging modalities such as X-ray and atomic force microscopy have been used to study the printed film morphology and material properties [5,6]. Due to their bulky nature, these techniques are expensive, slow, and almost impossible to carry out real-time in-situ measurements during the print process [7]. Similarly, infrared imaging and thermocouple have been used to measure the real-time temperature of the printing process in additive manufacturing [8]. These techniques have been quite successful for temperature measurement. However, they require complex setup and integration with the printing system. An ideal quality control system for PE should be compact, cheap, and operatable real-time with multi-sensing abilities. This would enable real-time feedback to the users allowing them to be aware of any potential print defects before print completion saving resources and time. This paper demonstrates a unique approach to monitoring the PE process using an ultrasonic imager.

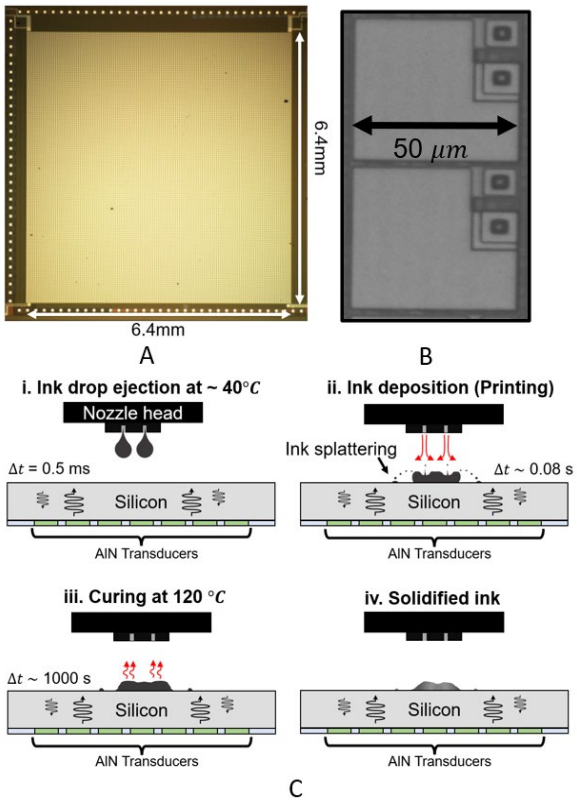

Figure 1. A) Optical image of the 128x128 AlN transducer pixels. B) Micrograph of 2 array pixels (50μm pitch) with integrated T/R circuits. C) Schematic showing ultrasonic imaging of ink printing process i) Ink drop ejection at warm ink temperature (~ 40°C). ii) Ink spreading on the surface causing few micro-drops to splatter. iii) Curing the deposited ink at 120 °C that evaporates the solvent. iv) Solidified ink on the imager surface.

The Geegah imager consists of 128 x 128 transmit/receive pixels with each pixel's pitch being 50 μm (Fig 1A). Each pixel has a 2 μm thick aluminum nitride (AlN) transducer, and most of the necessary circuitry is integrated within using a 130 nm CMOS process (Fig 1B), resulting in a compact, low-cost, low-power chip. The sensing region is the backside of the double-side-polished CMOS substrate with 6.4 x 6.4 mm^2. This optically flat, unobstructed surface without any wirebonds provides a rugged

surface that can be used for printing directly on it. The surface can be cleaned easily using solvent-soaked wipes multiple times without damaging the sensitive CMOS transistors or causing wear on encapsulation around wirebonds. During the ink printing process, high-frequency ultrasonic pulses are launched from these pixels, which then travel through the silicon substrate and are received back by the identical transducers (Fig 1C). The amplitude of these ultrasonic echoes is then used to form an image via the on-chip readout and signal processing circuitry [9]. At GHz frequency, the time taken for a pulse to be transmitted and received by a pixel is approximately 150 ns which enables capturing ink deposition at a very high scanning rate of 10-30 fps for the full 128x128 pixel array.

This ultrasonic (US) GHz imager has few key features that make it a suitable tool for PE quality control. Firstly, the high frequency in the GHz range allows for acquiring high-resolution images as frequency is inversely proportional to the wavelength. When operated at 1.85 GHz, the wavelength is around 4.5 μm in silicon. Secondly, the reflected ultrasonic signal magnitude and phase are used to simultaneously estimate the material's acoustic impedance and temperature data. This integration of multiple sensing modes on the same chip reduces the whole imaging system's power, size, space, and cost. Thirdly, the CMOS-MEMS integration enables additional GPS and RF communication features. This facilitates the users to monitor the print and receive data remotely. Fourthly, ultrasonic waves instead of light allow imaging transparent ink and features that remain hidden/covered during the print, and hence can't be sufficiently detected by optical approaches. Several print defects such as air bubbles and cracks between the substrate (imager surface) and the ink layer is clearly visible using the ultrasonic imager but not necessarily in optical images.

In previous work, we have demonstrated the use of the GHz ultrasonic imager array to sense nematodes [10], and soil parameters[11], based on CMOS integration of piezoelectric AlN transducers. Here, we show the potential of this technology for monitoring and optimization of ink-printing process parameters such as the density, temperature, and distance between the nozzle and the substrate.

METHODS AND EXPERIMENTS

The demonstration of real-time ultrasonic imaging of ink is done using the BotFactory SV2 inkjet printer. This printer utilizes a HP45 cartridge consisting of 300 thermal inkjet nozzles with a firing rate of approximately 2 kHz. A plate inside the nozzle chamber rapidly heats up, boiling the ink causing vapor formation and pressure that pushes the ink towards the extruder. The vapor bubble grows and ruptures that pinches off ink droplet out of the extruder. Due to the surface tension, the excess ink contracts and flows back into the chamber waiting for the next ejection cycle. Conductive ink was used for all the printing experiments in this paper, although results on non-conductive and resistive inks are also possible. This conductive ink consists of a matrix of silver nanoparticles suspended in a solvent. For complete adhesion of the ink on a substrate, thermal curing at a temperature of 120-150 °C is required. This heating causes the solvent to evaporate, leaving behind the silver particles attached to the substrate. The printer has a XYZ step resolution of 10 microns and minimum trace width of 200 µm. The operating temperature of the bed, on which the imager is mounted on, ranges from 25 – 150 °C. Therefore, it is important that the imager can operate at high temperatures.

The GHz imager chip was placed parallel to the printer bed, and Kapton tape was used to secure the PCB with the imager chip in the fixed location to prevent any movements during the printing process (Fig. 2A). A pattern of varying line widths was directly printed on the imager's surface (Fig. 2B). For all experiments, pulse

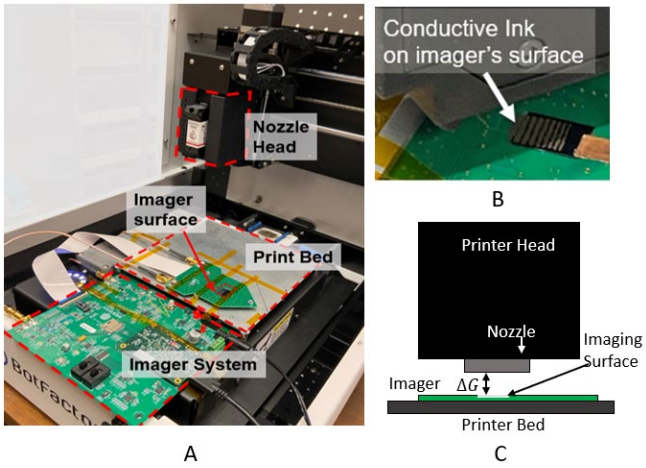

Figure 2.A) Experimental setup of imager chip attached parallel to the SV2 printer's bed. B) Conductive ink deposited on the imager's surface during the print. C) Schematic showing experiment varying gap between nozzle and the imager surface.

frequency used to image the ink was 1.853 GHz, and the sampling rate for the experiments was approximately 5.8 frame per second (fps). The 3D printer's bed temperature was set to 50 °C, whereas the curing was performed at 120 °C. The imager was initially calibrated to measure temperature change of the pixels. This was done by placing the chip inside an environment chamber (Tenny Environmental TJR) and imaging air with 1.853 GHz ultrasound for varying temperatures(-10 to 120 °C). The calibration curve obtained was used to measure the ink printing and curing temperature.

A series of experiments were performed to optimize the distance between the nozzle and substrate. The same line pattern was directly printed on the surface in multiple experiments where only the gap between the imager's surface and the nozzle (**Δ**G) was varied from 4.5 mm to 7.0 mm (Fig 2C). The obtained ultrasonic images were analyzed to quantify the ink splattering and print precision.

RESULTS AND DISCUSSION

The reflected echo from each pixel is received in two modes – in phase (I) and out-of-phase (Q). When imaging with all the pixels, two 128 x 128, 12-bit matrices for I and Q data are generated. These matrices ($\boldsymbol{I_M}$ and $\boldsymbol{Q_M}$) contain the first acoustic echo signal reflected from the backside of the silicon. The background noise is removed from the images by subtracting the measured echo matrices with the air-backed echo ($\boldsymbol{I_B}$ and $\boldsymbol{Q_B}$) thus obtaining the following matrices:

$$\boldsymbol{I_{Image}} = \boldsymbol{I_M} - \boldsymbol{I_B} \quad (1)$$

$$\boldsymbol{Q_{Image}} = \boldsymbol{Q_M} - \boldsymbol{Q_B} \quad (2)$$

The no-echo signal is also sampled after the first echo dies off and before the second echo. The obtained data ($\boldsymbol{I_N}$ and $\boldsymbol{Q_N}$) are used to remove any DC offsets from the images. The two important components of reflected echo are the magnitude and phase. The magnitude represents the intensity of the wave, whereas the phase measures any doppler shift of frequency. Using the I and Q echo/no-echo measurements, magnitude and phase can be calculated as follows:

$$\text{Magnitude} = \sqrt{(\boldsymbol{I_M} - \boldsymbol{I_N})^2 + (\boldsymbol{Q_M} - \boldsymbol{Q_N})^2} \quad (3)$$

$$\text{Phase} = \boldsymbol{\tan^{-1}}\left(\frac{\boldsymbol{I_M} - \boldsymbol{I_N}}{\boldsymbol{Q_M} - \boldsymbol{Q_N}}\right) \quad (4)$$

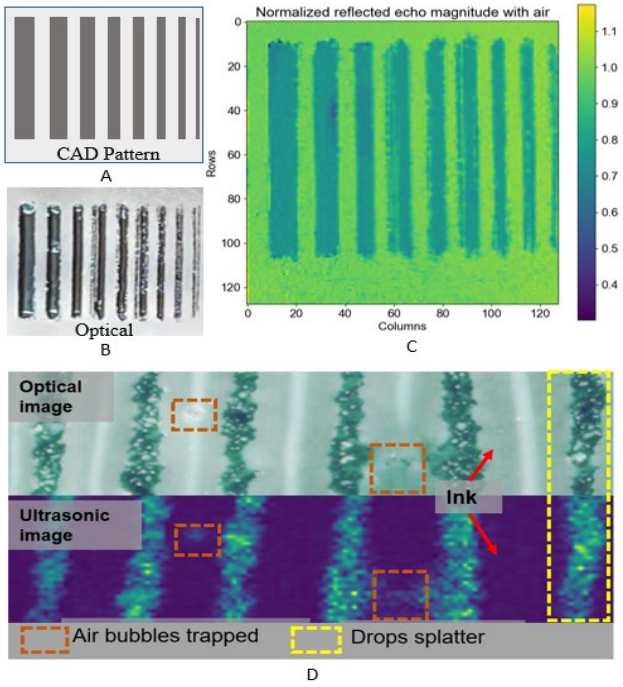

Figure 3.A) CAD pattern (grey area shows ink) for printed conductive ink lines. B) Optical image of the printed conductive ink on the imager surface. C) Ultrasonic image of the same ink patterns. D) Optical and ultrasonic images showing defects in the ink print pattern: air bubbles trapped within ink and tiny drops splattering between the ink lines.

For consistent comparison of the calculated magnitude among different experiments, the magnitude of the measured signal is normalized with the magnitude of baseline using the following relationship:

$$\text{Normalized magnitude} = \frac{\boldsymbol{Magnitude\_Measured}}{\boldsymbol{Magnitude\_Baseline}} \quad 5)$$

Ultrasonic images of ink printing and curing

The CAD implemented design, optical image, and the magnitude echo of the reflected signal (Fig 3 A,B,C respectively) shows the line patterns deposited on the imager chip. The ultrasonic and optical images (Figure 3 D) reveal print defects such as cracks, trapped air bubbles, and ink splattering on the imager surface. As only a single layer of ink was deposited, the flaws are visible on both imaging modalities. However, ultrasonic imaging would have a significant advantage, especially with transparent ink that is hard to image optically and multi-layered prints where the bottom layer remains hidden due to the top layers.

Temperature Sensing and ink curing

The silicon substrate of the GHz imager makes temperature sensing possible as the change in the speed-of-sound in silicon with temperature manifests as a phase shift in the ultrasonic signal received by the imager pixel transducers [12]. The relationship between the unwrapped phase measured for varying air temperature (-10 to 120 °C) is linear (Fig 4A). Using this calibration curve, the temperature for ink drop deposition was interpolated from 18 pixels (Fig 4B). Here, the temperature can be seen dropping after the liquid delivery as locally heat is removed from the silicon to heat the droplet. The ink can be also seen to spread enabling measurement of spreading in real time. Eventually, the ultrasonically measured temperature slowly returns to the ambient temperature as the ink reaches thermal equilibrium with the substrate. Similarly, the temperature change was recorded from 8 pixels exposed to ink during the curing process (Fig 4C). Although the print bed is measured to be approximately 120° C, the pixel temperature is lower ~ 110 °C due to the rapid heat transfer to the surrounding air and the placement of the imager onto the print surface.

Varying the height between the nozzle and substrate

The distance between the nozzle and substrate affects ink drop breakage properties such as breaking time and rate during ejection, resulting in ink splattering [13]. The reflected echo magnitude

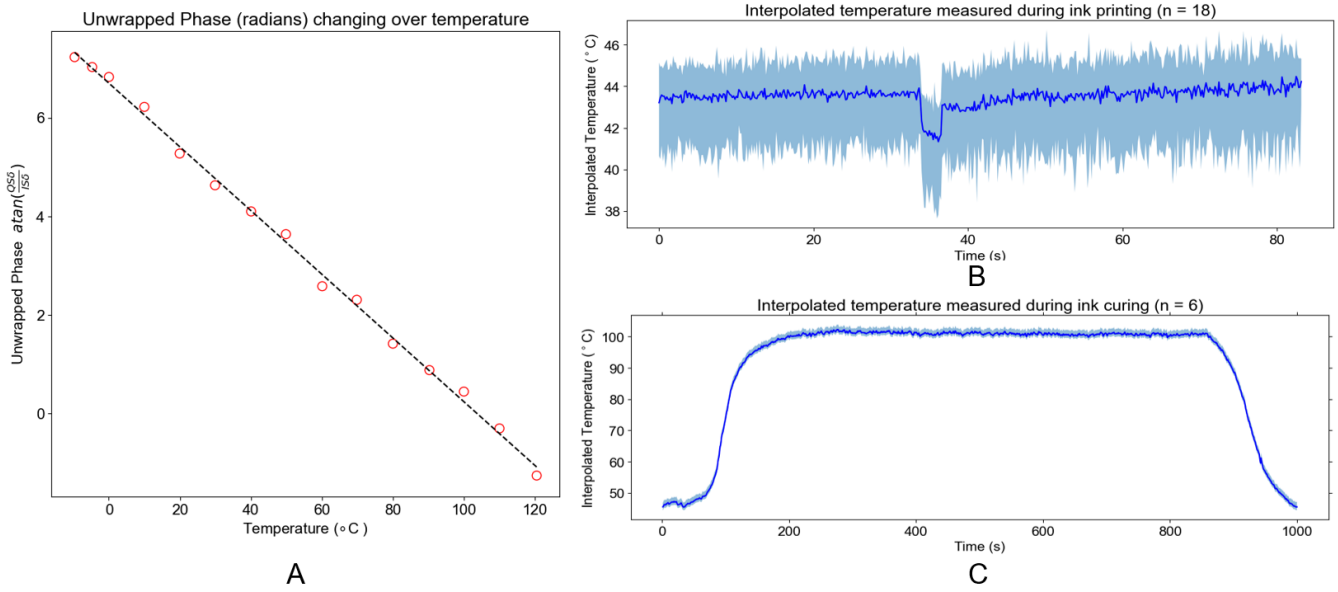

Figure 4. A) Calibration curve showing linear relationship between the calculated unwrapped phase and temperature. B) Interpolated temperature measurement of ink printing. Ink temperature is cooler than the imager surface causes the temperature to drop briefly. C) Interpolated temperature for ink curing. The shadow represents the maximum and minimum values among the measured data.

images (Fig 5A) reveal increasing ink splattering around the printed lines as the gap increases. The splattering was further quantified by plotting the distribution of the signal from all the pixels (Fig 5B). The lower splattering of micro-sized drops results in clear-distinct peaks of signals reflected from air and ink pixels. In contrast, high splattering causes the air gaps to be filled with tiny drops of ink, resulting in broader distribution. This quantification of the ink splattering can optimize the proper height between the nozzle and the substrate to have the least ink splattering.

CONCLUSION

This work demonstrates the GHz ultrasonic imager as a potential tool for quality control in PE manufacturing. Ultrasonically imaging the ink deposition and curing yields crucial data on ink's acoustic impedance and temperature that can be used to predict any anomalies or faults in the prints. In future experiments, the images obtained from the US imager can be correlated with optical images and functional data obtained on FR4/Kapton/Polyimide substrates, using AI/ML approaches to have an automated feedback PE manufacturing process. In addition, different ink types such as resistive and insulating ink will also be imaged to characterize their acoustic properties. This model may help predict ink aging or substrate properties that can be used to provide a sub-optimal print. This capability will specially be useful for printed electronics in adverse environments such as on mobile platforms experiencing temperature, humidity, and vibration variations during the print. The models correlating ultrasonic images to the actual prints may also determine optimum inkjet operating parameters such as distance from the substrate, firing rates of each nozzle, and misfiring nozzles that should not be used in a print. This level of feedback control will enable high yields and greater ink use efficiency, reducing the cost of printed electronics devices. In the future, the imager can be directly integrated with the PE printer for automatic sampling and process optimization of the printing and curing processes.

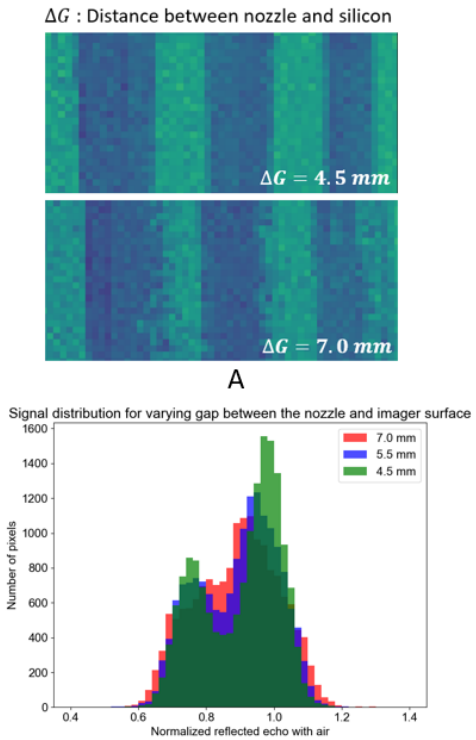

Figure 5. A) Ultrasonic images reveal precise and distorted lines printed for smaller (4.5 mm) and larger gaps (7.0 mm), respectively. B) Distribution of ultrasonic echo amplitude divided into two peaks for varying gap between nozzle and imager surface. A smaller gap causes less splattering, which leads to more distinct peaks.

ACKNOWLEDGEMENTS

This work was performed in part at the Cornell NanoScale Facility, an NNCI member supported by NSF Grant NNCI-2025233. This material is based on research sponsored by Army Research Laboratory under agreement number W911NF-19-2-0345. The U.S. Government is authorized to reproduce and distribute reprints for Government purposes notwithstanding any copyright notation thereon. The views and conclusions contained herein are those of the authors and should not be interpreted as necessarily representing the official policies or endorsements, either expressed or implied, of Army Research Laboratory (ARL) or the U.S. Government.

REFERENCES

[1] S. K. Garlapati et al., "Printed Electronics Based on Inorganic Semiconductors: From Processes and Materials to Devices," Advanced Materials, vol.30, no. 40, p.1707600, Jun. 2018

[2] J. Chang et al., "Challenges of printed electronics on flexible substrates," 2012 IEEE MWSCAS Aug. 2012

[3] M. Mantysalo et al., "Capability of inkjet technology in electronics manufacturing," 2009 59th Electronic Components and Technology Conference, May 2009

[4] Beedasy, V., & Smith, P. J. (2020). Printed Electronics as Prepared by Inkjet Printing. Materials, 13(3), 704

[5]J. Rivnay et al., "Large modulation of carrier transport by grain-boundary molecular packing and microstructure in organic thin films," Nature Materials, vol. 8, no. 12, pp. 952–958, Nov. 2009

[6] R. J. Kline, M. D. McGehee, E. N. Kadnikova, J. Liu, J. M. J. Fréchet, and M. F. Toney, "Dependence of Regioregular Poly(3-hexylthiophene) Film Morphology and Field-Effect Mobility on Molecular Weight," Macromolecules, vol. 38, no. 8, pp. 3312–3319, Apr. 2005

[7] F. Pastorelli, N. Accanto, M. Jørgensen, N. F. van Hulst, and F. C. Krebs, "In situ electrical and thermal monitoring of printed electronics by two-photon mapping," Scientific Reports, vol. 7, no. 1, Jun. 2017

[8] P. K. Rao, J. (Peter) Liu, D. Roberson, Z. (James) Kong, and C. Williams, "Online Real-Time Quality Monitoring in Additive Manufacturing Processes Using Heterogeneous Sensors," Journal of Manufacturing Science and Engineering, vol. 137, no. 6, Sep. 2015

[9] M. Abdelmejeed et al., "Monolithic 180nm CMOS Controlled GHz Ultrasonic Impedance Sensing and Imaging," 2019 IEEE IEDM, Dec. 2019,

[10] J. Kuo et al., "Gigahertz Ultrasonic Imaging of Nematodes in Liquids, Soil, and Air," 2021 IEEE IUS, Sep. 2021

[11] A. Baskota et al., "Gigahertz Ultrasonic Multi-Imaging of Soil Temperature, Morphology, Moisture, and Nematodes," 2022 IEEE MEMS, Jan. 2022

[12] M. Abdelmejeed et al., "A CMOS compatible GHz ultrasonic pulse phase shift-based temperature sensor," 2018 IEEE MEMS, Jan. 2018

[13] J. Park, et al., "Methodology to set up nozzle-to-substrate gap for high resolution electrohydrodynamic jet printing," Applied Physical Letters, vol. 109, no. 13, p. 134104

CONTACT

Anuj Baskota, *anuj@geegah.com